

Supplemental Information

Ultrahigh energy storage capability of trilayer polyetherimide/poly(vinylidene fluoride-trifluoroethylene- chlorofluoroethylene) with low loading of boron nitride nanosheets

Huijian Ye, Huilei Jiang, Lixin Xu*

College of Materials Science and Engineering, Zhejiang University of Technology,
Hangzhou 310014, China

* Corresponding author, E-mail: gcsxlx@zjut.edu.cn (L. Xu)

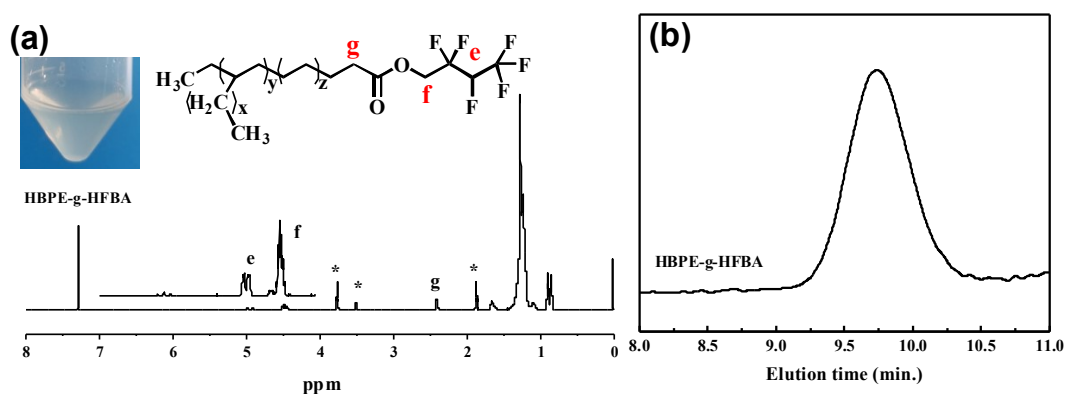


Figure S1. The structural characterizations of HBPE-g-HFBA copolymer: (a) ¹H NMR spectra, and (b) GPC trace.

Table S1. The grafting characterizations and GPC results of HBPE-g-HFBA

Sample	Volume (mL)	Yields (g)	HFBA grafting ^a (mol%)	Branching degree ^b (/1000C)	GPC ^c		
					$\bar{M}_{n,PS}$ (kD)	$\bar{M}_{w,PS}$ (kD)	PDI
HBPE-g-HFBA	20	3.88	4.3	84.2	27.8	33.4	1.2

a: HFBA grafting obtained via ¹H NMR spectroscopy based on end-group analysis.

b: Degree of branching determined via ¹H NMR spectroscopy.

c: Number-averaged molecular weight (M_n), weight-averaged molecular weight (M_w)

and polydispersibility index (PDI) determined via GPC with polystyrene (PS) standards.

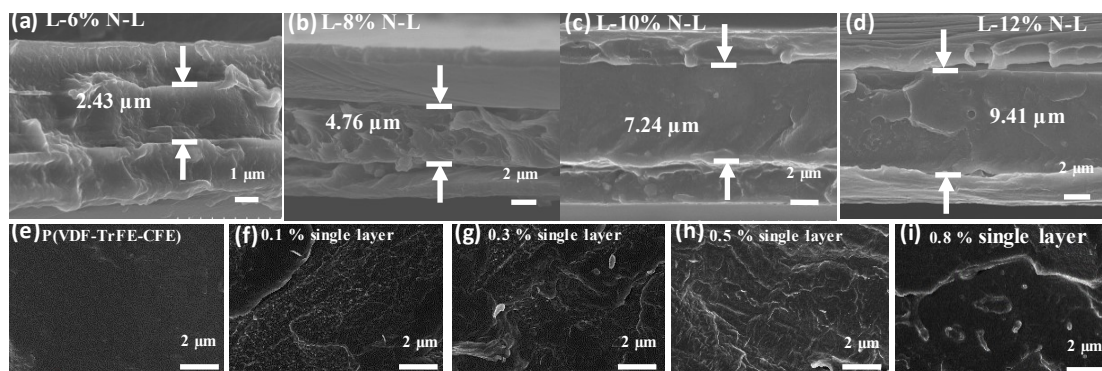


Figure S2. Cross-sectional SEM morphology of trilayer all-polymer LNL composite and BNNs/P(VDF-TrFE-CFE) nanocomposite.

Table S2. Layer thickness and volume fraction of trilayer all-polymer LNL composites with different P(VDF-TrFE-CFE) loadings

	Concentration (wt%)	P(VDF-TrFE-CFE) thickness (μm)	PEI thickness (μm)	P(VDF-TrFE-CFE) (vol%)
L-6%N-L	6	2.4		33.3
L-8%N-L	8	4.7	2.4	49.5
L-10%N-L	10	7.2		60
L-12%N-L	12	9.4		66.2

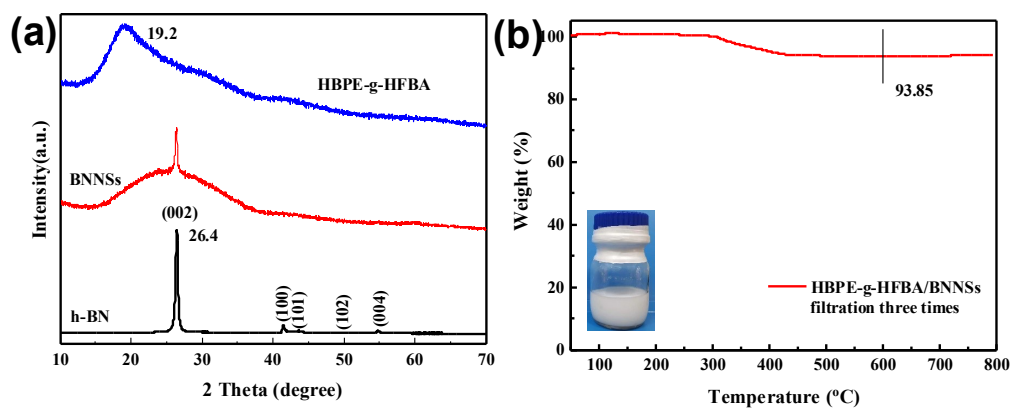


Figure S3. (a) XRD patterns, and (b) TGA curves of BNNs.

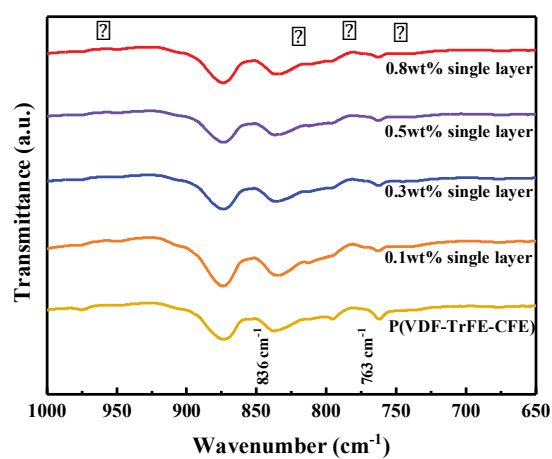


Figure S4. FTIR spectra of BNNs/P(VDF-TrFE-CFE) nanocomposite.

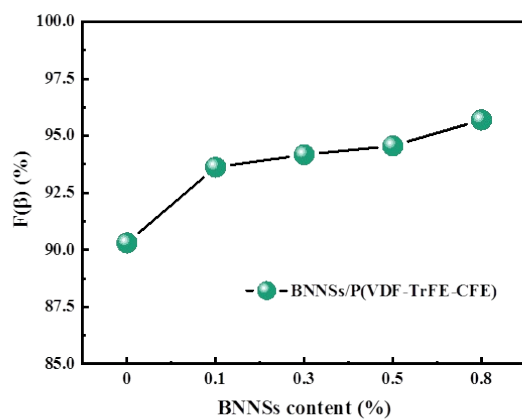


Figure S5. Relative content of β-phase in BNNs/P(VDF-TrFE-CFE) nanocomposite determined by FTIR spectroscopy.

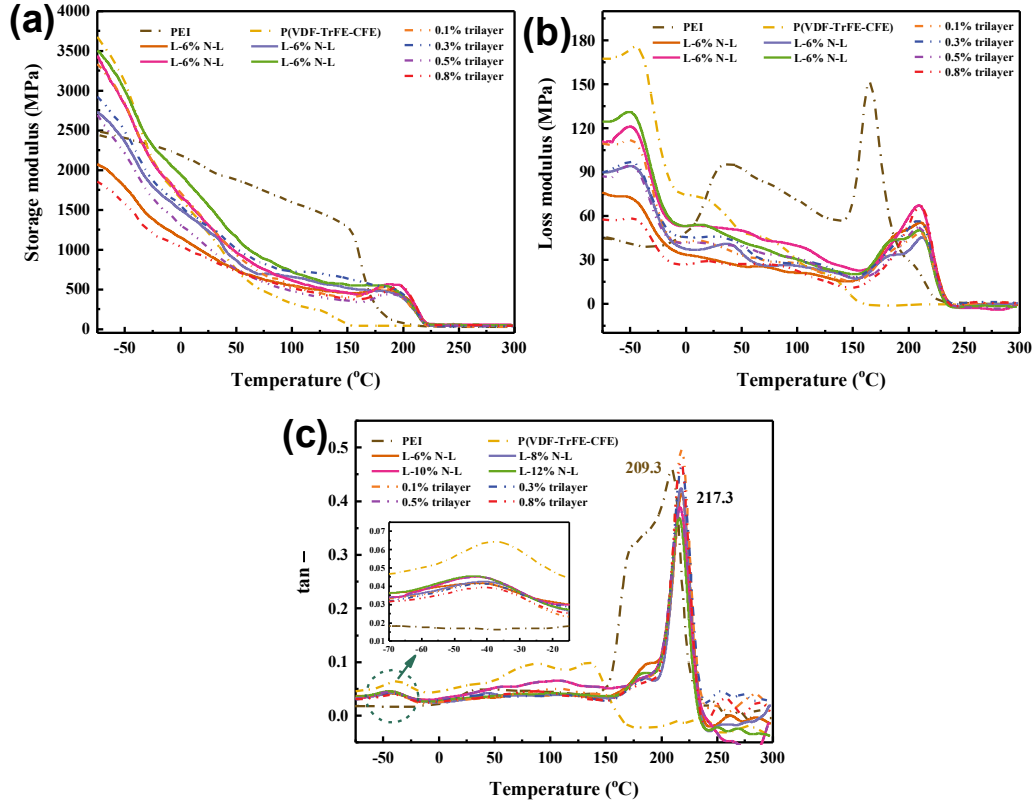


Figure S6. Dynamic thermomechanical analysis of composite (a) storage modulus, (b) loss modulus, and (c) loss factor.

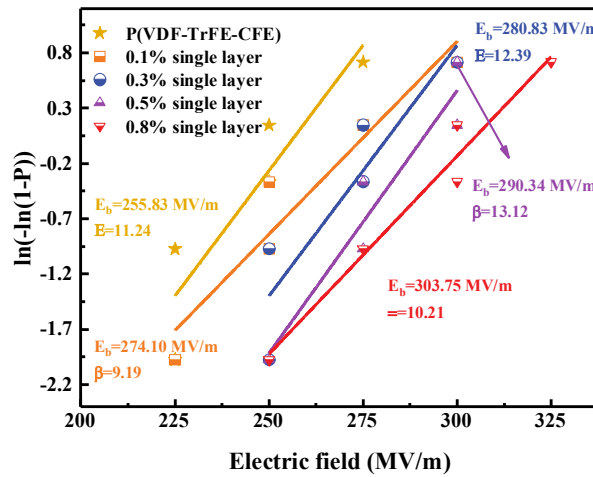


Figure S7. Two-parameter Weibull distribution plots of monolayer composite.

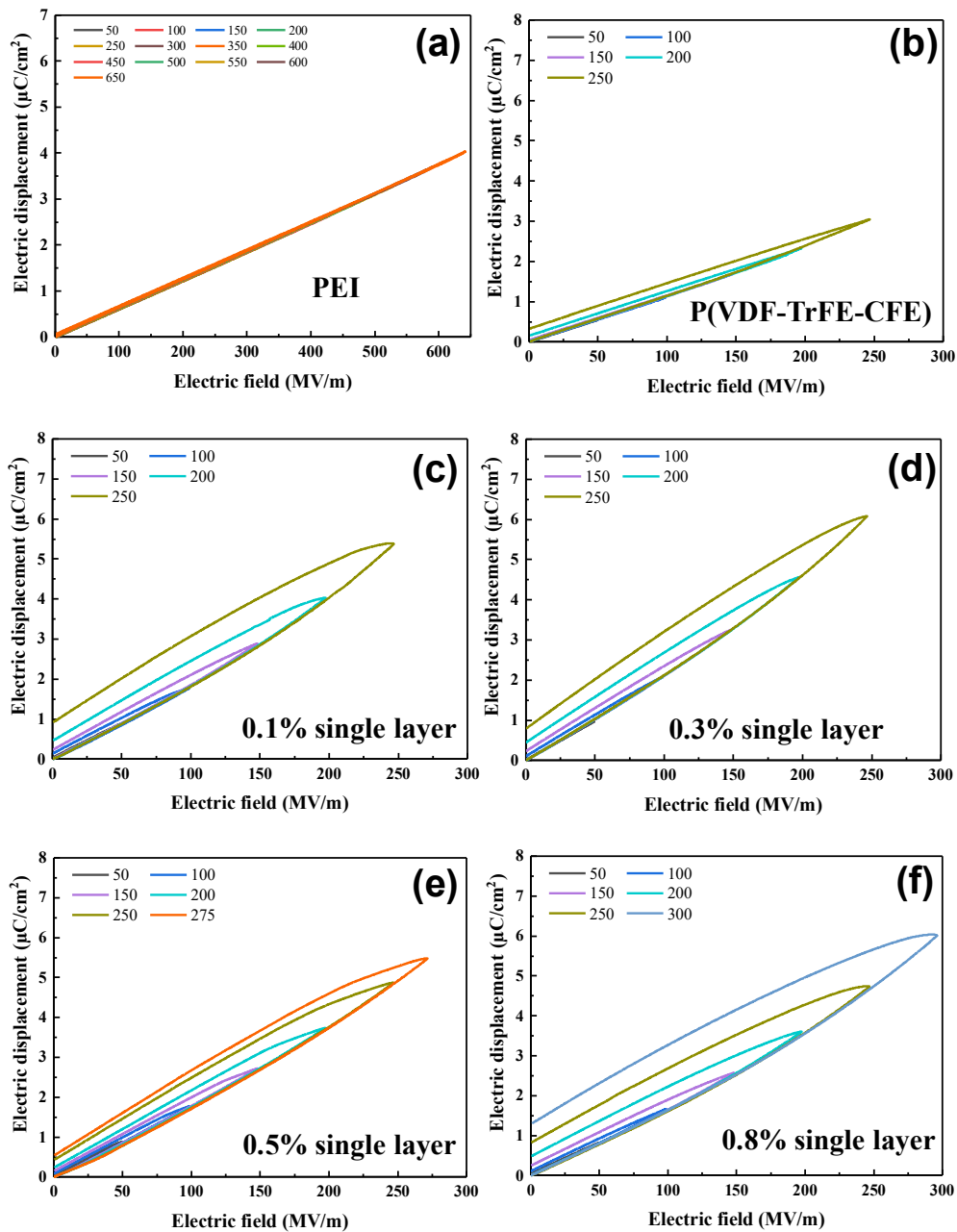


Figure S8. The unipolar P-E loops of monolayer films: (a) pure PEI, (b) pure P(VDF-TrFE-CFE), (c) 0.1% composite, (d) 0.3% composite, (e) 0.5% composite, and (f) 0.8% composite.

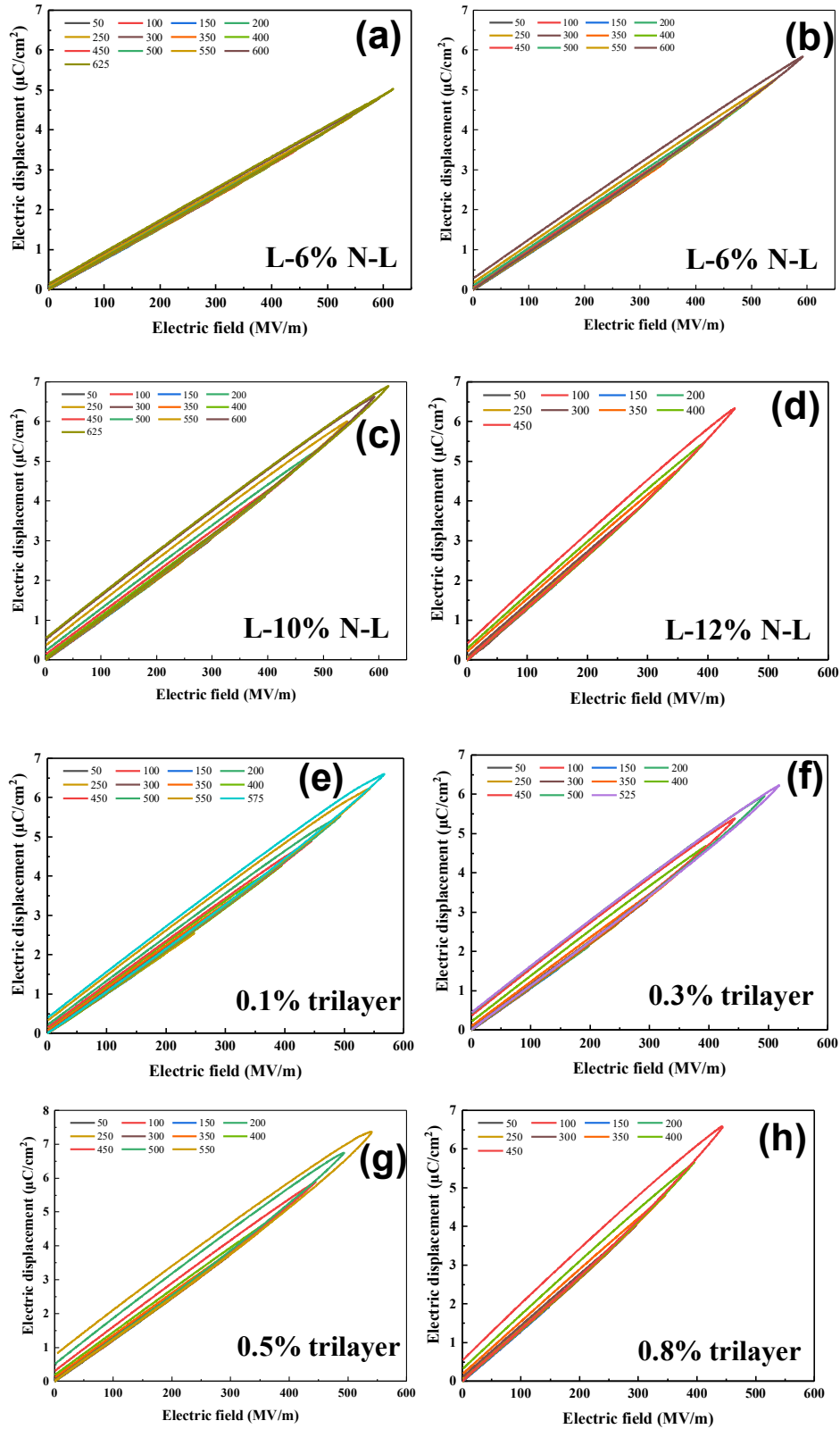


Figure S9. The P-E loops of all-polymer trilayer films: (a) L-6%N-L, (b) L-8%N-L, (c) L-10%N-L, (d) L-12%N-L. The P-E loops of BNNs/LNL films with different BNNs mass fractions: (e) 0.1%, (f) 0.3%, (g) 0.5%, and (h) 0.8%.

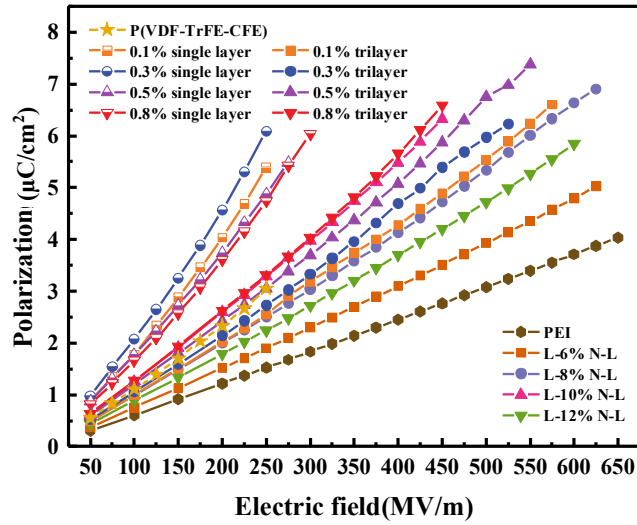


Figure S10. Maximum electrical displacements of pure PEI, pure P(VDF-TrFE-CFE), monolayer and trilayer composites.

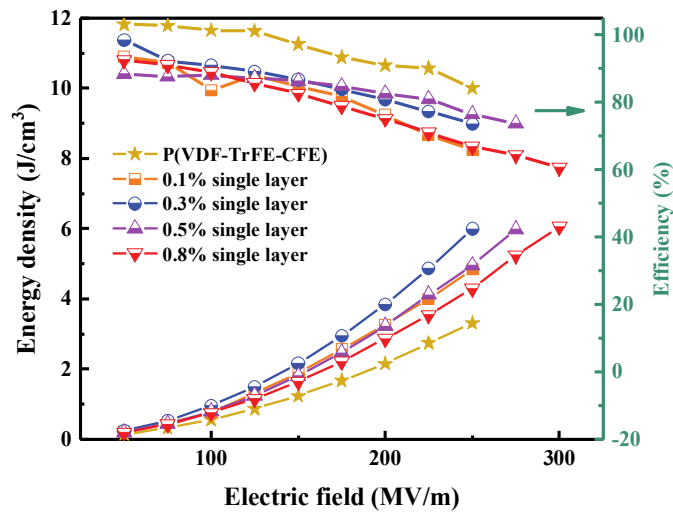


Figure S11. Energy density and charge-discharge efficiency of BNNSs/P(VDF-TrFE-CFE) composite.